Applied Physics Letters ARTICLE pubs.aip.org/aip/apl

Giant static refractive index gradient induced by strong ultrasonic wave

Cite as: Appl. Phys. Lett. **124**, 011102 (2024); doi: 10.1063/5.0174915
Submitted: 4 September 2023 · Accepted: 13 December 2023 ·
Published Online: 2 January 2024

View Online Export Citation CrossMark

Yuki Harada,[1] Mutsuo Ishikawa,[2] Yuma Kuroda,[1] Mami Matsukawa,[1] and Daisuke Koyama[1,a)]

AFFILIATIONS

[1]Faculty of Science and Engineering, Doshisha University, 1-3 Tataramiyakodani, Kyotanabe, Kyoto 610-0321, Japan
[2]Faculty of Biomedical Engineering, Toin University of Yokohama, 1641 Kurokane, Aoba, Yokohama, Kanagawa 225-8503, Japan

[a)]Author to whom correspondence should be addressed: dkoyama@mail.doshisha.ac.jp

ABSTRACT

Spatiotemporal modulation of refractive index in an optical path medium allows for control of light propagation. This refractive index change (Δn) can be achieved by external stimulation such as temperature or density change, but there is a limit to the extent to which Δn can be controlled by external stimulation acting on a single medium. Here, we demonstrate a technique to form a giant refractive index gradient ($\Delta n = 0.06$) in a small region of water (< 10 mm) using a high-frequency, high-intensity (in the 100-megahertz-range, on the order of megapascals) ultrasonic wave. Ultrasonic radiation in water can statically modulate the refractive index in water from the initial value ($n = 1.33$) toward that of air.

Waves such as those of light and sound tend to propagate toward spaces with a slower propagation speed, i.e., with a higher refractive index for light. This means that to control light in an optically uniform medium without using lenses or mirrors, it is necessary to change the refractive index distribution of the field in which the light propagates. One method for spatiotemporal control of light is to modulate the physical properties of the propagation medium, i.e., by alteration of refractive index using external stimulation such as applied pressure variation, applied electromagnetic forces, or temperature change. The refractive indices of media are dependent on pressure, meaning that periodic vibrations, such as ultrasonic waves propagating through a medium, provide a promising method for controlling light. Furthermore, the use of ultrasonic waves allows the refractive index of the medium to be changed instantaneously in optical control techniques. The interaction between light and ultrasonic waves has long been known as an acousto-optic (AO) effect, and AO devices such as AO modulators and deflectors employ Bragg diffraction and Raman–Nath diffraction.[1,2] Tunable acoustic gradient (TAG) index lenses have also been developed, in which the refractive index distribution within the lens is periodically changed by high-intensity ultrasonic waves, allowing high-speed, precise optical focus sweeps with high spatiotemporal resolution.[3,4] However, these AO devices utilize refractive index gradients synchronized with the temporal period and spatial wavelength of the ultrasonic waves, and do not refract and reflect the light statically as conventional lenses or mirrors do. In addition, the refractive index change (Δn) caused by these AO devices is very small (Δn on the order of 10^{-4} to 10^{-5}).[5] Although typical AO devices use the periodic change in refractive index induced by ultrasonic waves, we have previously devised and demonstrated a method to modulate refractive index using the static radiation force of ultrasonic waves[6,7] and developed variable-focus lenses[8–10] that can statically refract light using this technique.

In this Letter, we experimentally demonstrate that a static change in refractive index (Δn on the order of 10^{-2}) is formed in a small region (<10 mm) when a liquid is radiated by high-frequency high-intensity (in the 100-megahertz-range, on the order of megapascals) ultrasonic waves. There are no previous reports in the literature of a technique that can statically control the refractive index in a single medium, over a wide range, using ultrasonic waves. This technique, using high-frequency high-intensity ultrasonic waves, enables spatiotemporal control of light at the microscale and may be widely applicable in technologies such as gradient index lenses for endoscopic biomedical imaging,[11–13] optical waveguides,[14–16] and optofluidic sensing devices for lab-on-chip technologies.[17,18]

The high-frequency, high-intensity ultrasonic transducer is fabricated using a $KNbO_3$ piezoelectric film (with thickness of approximately 70 μm) grown by the hydrothermal method at 240 °C on a (100)c Nb-$SrTiO_3$ substrate.[19] A layout of the experimental system used for laser beam deflection is shown in Fig. 1(a). We place the $KNbO_3$ ultrasonic transducer [Fig. 1(b)] in a glass cell ($10 \times 10 \times 45$ mm^3) filled with

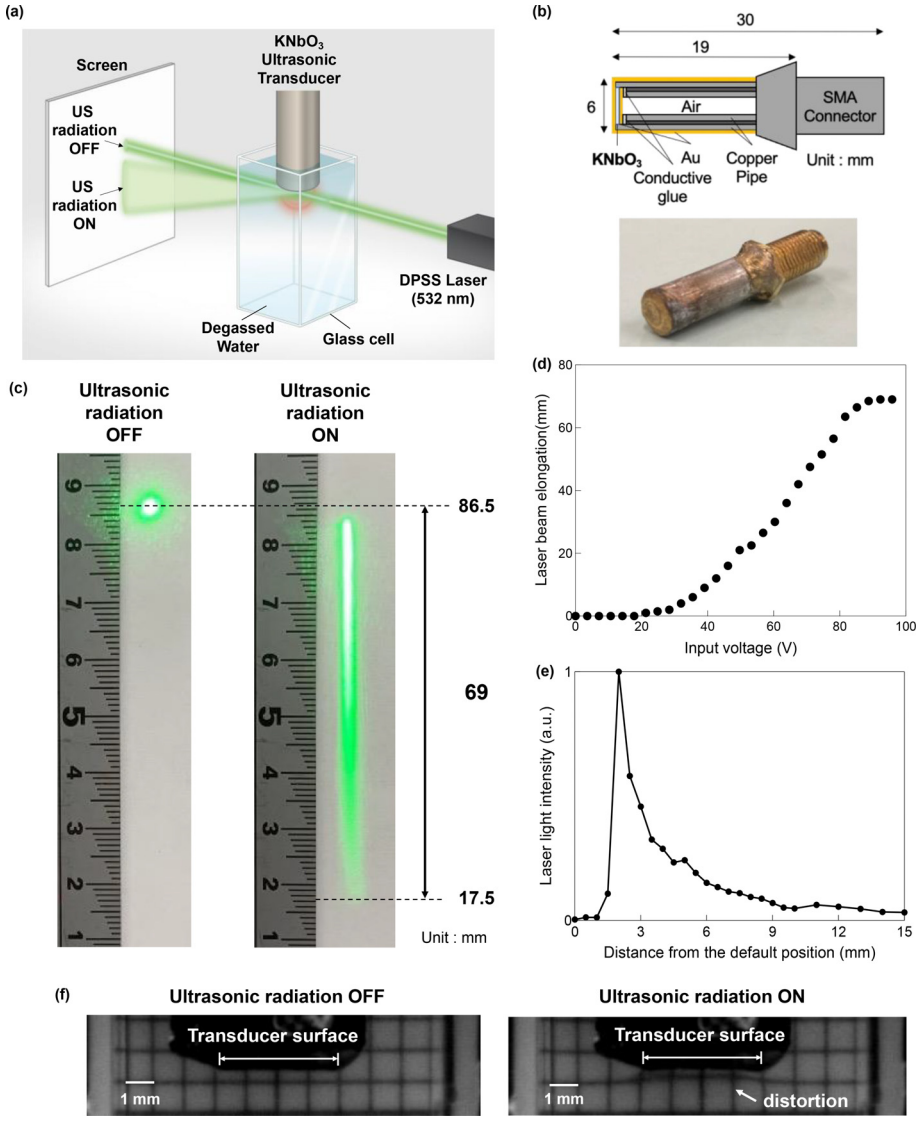

FIG. 1. Laser beam deflection induced by high-frequency, high-intensity ultrasonic waves in water. (a) Experimental setup for laser beam deflection. (b) Structure and photograph of $KNbO_3$ piezoelectric transducer. (c) Laser beams projected on the screen without and with ultrasonic radiation (160 MHz, 92 V_{pp}). The high-frequency, high-intensity ultrasonic waves in water cause elongation of the laser beam in the sound-axis (ultrasonic wave propagation) direction. (d) Relationship between input voltage to the ultrasonic transducer and the laser beam elongation. (e) Light intensity distribution of the laser beam in the case with the laser beam elongation of 15 mm. (f) Photograph of the spatial distribution of the refractive index change (Δn) caused by high-frequency, high-intensity ultrasonic wave radiation (160 MHz, 92 V_{pp}) using a high-speed camera and a grid-patterned panel.

degassed water. Linearly polarized light from a continuous wave (CW) diode-pumped solid-state laser (wavelength 532 nm, incident laser intensity of 0.73 mW) is passed through a pinhole with a diameter of 1 mm at an incident perpendicular to the sound-axis of the ultrasonic waves transmitted from the transducer. A continuous sinusoidal electric signal at a frequency of 160 MHz, generated by a function generator (T3AFG500, Teledyne Technologies), is amplified to 51 dB using a high-frequency amplifier (A1020-75-250, Hubert) to excite the $KNbO_3$ ultrasonic transducer. A screen is placed perpendicular to the central axis of the ultrasonic transducer at a distance of 735 mm to observe the light pattern of the laser beam affected by the ultrasonic field in the cell. Figure 1(c) shows a representative result of the laser beam deflection by high-frequency, high-intensity ultrasonic waves (160 MHz, transducer input voltage 92 V_{pp}, where V_{pp} is the maximum to minimum voltage amplitude) observed on the screen. The position of the laser beam is shifted from the position of 86.5 mm [US radiation OFF in Fig. 1(c)] to 84.5 mm [US radiation ON in Fig. 1(c)] on the screen, and its shape is elongated to approximately 69 mm in the direction toward the sound-axis, meaning that the high-frequency high-intensity ultrasonic waves induce a change in the refractive index in water (supplementary material, movie 1). In the linear region with low-intensity ultrasonic waves, the AO effect based on the interaction between light and high-frequency ultrasonic waves in the 100 MHz range is dominated by Bragg diffraction, while the high-frequency, high-intensity ultrasonic waves in the nonlinear region show different behavior. Considering the deflection angle of the laser beam, the refractive index of water near the surface of the transducer was smaller than that under atmospheric pressure ($n = 1.33$). Figure 1(d) shows a change in the elongation of laser beam in the sound-axis direction with a change in the input voltage to the ultrasonic transducer. Although the laser beam on the screen shows no change below a threshold transducer voltage of 21 V_{pp}, it begins to elongate at input voltages greater than 21 V_{pp}, and the elongation increases

nonlinearly with input voltage. It is clear that the refractive index in water changes gradually along the sound-axis direction, caused by the high-frequency, high-intensity ultrasonic waves, and that the change in refractive index depends on the sound pressure amplitude. The time constant τ at a position 10 mm down from the initial beam spot [76.5 mm in Fig. 1(c)] is approximately 1.53 s when the laser beam is elongated in the sound-axis direction by ultrasonic radiation (160 MHz, 63 V_{pp}). Figure 1(e) shows the light intensity distribution of the laser beam in the case with the laser beam elongation of 15 mm. The laser beam transmitted through a 0.5 mm pinhole was measured by an optical power meter (Model 843-R, Newport, MA, USA). The laser light intensity decreased exponentially in the range of 2–15 mm. Having confirmed the optical deflection of laser light in the above-mentioned experiments, we verify the spatial distribution of Δn caused by high-frequency high-intensity ultrasonic wave radiation (160 MHz, 92 V_{pp}) using a high-speed camera and a grid-patterned panel. Figure 1(f) shows that the lines of the grid in the image are distorted toward the ultrasonic transducer surface, where the laser beam is deflected by the ultrasonic waves (supplementary material, movie 2). This shows a trend that is similar to the previous results [Fig. 1(c)], and supports the possibility of static negative Δn in water by high-frequency high-intensity ultrasonic waves.

Next, we use schlieren photography with a high-speed imaging system to visualize the effect of Δn near the surface of the ultrasonic transducer.[20] This method uses the change in refractive index and the trajectory of light due to ultrasonic wave propagation, showing the distribution of Δn as a brightness distribution in the captured image. Figures 2(b)–2(d) show schlieren images around the tip of the $KNbO_3$ ultrasonic transducer radiating high-frequency high-intensity ultrasonic waves (160 MHz, 57 V_{pp}) (supplementary material, movie 3). Comparing the schlieren images without [Fig. 2(a)] and with [Fig. 2(b)] ultrasonic radiation, the refractive index of water near the transducer surface shows a clear change (white to black in the images) due to ultrasonic radiation. The Δn distribution in water reaches a steady state approximately 5.4 s after ultrasonic radiation commences at $t = 0$ s. The maximum size of the induced Δn distribution is approximately 6.4 mm in the radial (horizontal) direction and 1.3 mm in the sound-axis (vertical) direction of the transducer. When ultrasonic radiation ceases, the distribution of Δn diminishes gradually and disappears completely after approximately 3.9 s. It should be noted that a small gap is observed between the transducer surface and Δn distribution after 2.4 and 3.3 s [Figs. 2(c) and 2(d)] in the transient state. Additionally, during ultrasonic radiation, interference fringes with an interval of approximately 0.1 mm appear in the surrounding area of the distribution with a large Δn, as shown in Figs. 2(b)–2(d). These interference fringes are not observed without ultrasonic radiation, and will be further investigated in our future work.

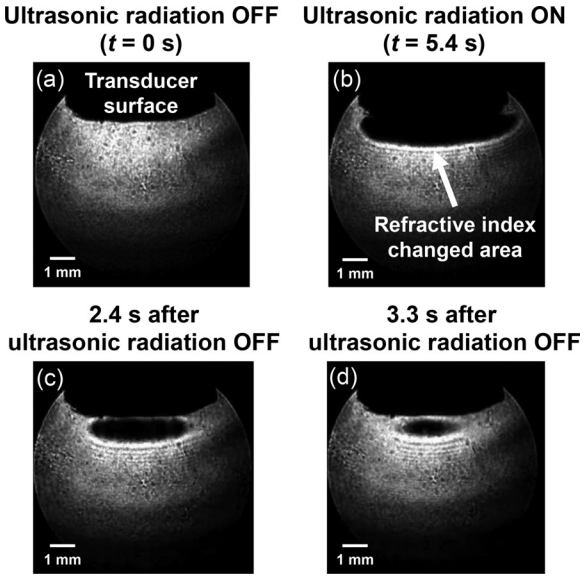

FIG. 2. Refractive index changes (Δn) induced by high-frequency, high-intensity ultrasonic waves, visualized using schlieren photography. (a) Schlieren image before ultrasonic radiation ($t = 0$ s). The ultrasonic transducer appears black. (b) Schlieren image at steady state ($t = 5.4$ s) under ultrasonic radiation at 160 MHz and 57 V_{pp}. The distribution of Δn by ultrasonic waves appears black near the ultrasonic transducer surface. (c) Schlieren image captured at 2.4 s after stopping ultrasonic radiation from the steady state. (d) Schlieren image captured at 3.3 s after stopping ultrasonic radiation from the steady state.

Direct measurement of the change in refractive index using a fiber optic probe is helpful for quantitative evaluation.[21–23] The $KNbO_3$ piezoelectric transducer is placed in an acrylic tank (200 × 200 × 200 mm^3) filled with degassed water, and high-frequency high-intensity ultrasonic waves are transmitted into the water. A single-mode optical fiber (P1-SMF28E-FC-2, Thorlabs, NJ, USA; core diameter: 10 μm; cladding diameter: 125 μm) is employed to measure Δn. The incident light from an amplified spontaneous emission (ASE) light source is reflected at the fiber tip and detected by a photoreceiver (MODEL 2053, Newport, MA, USA) via a circulator (6015-3-FC, Thorlabs, NJ, USA). A frequency-variable filter (FV-628B, NF Corporation, Kanagawa, Japan) removes electrical signals 1 Hz above the output signal, and the DC electrical signal is measured using a digital oscilloscope (MSO54B, Tektronix, OR, USA) [Fig. 3(a)]. We observe the change in DC signal without and with ultrasound radiation to evaluate the static change of Δn. The Fresnel reflectance from the tip surface of the optical fiber depends on the refractive index difference between the optical fiber (glass) and the surrounding medium (water), making it possible to measure the local Δn in the water.[23] In the absence of ultrasonic waves, the reflection ratio of the light intensity R_{off} at the tip surface of the optical fiber is expressed as

$$R_{off} = \left(\frac{n_f - n_w}{n_f + n_w}\right)^2, \tag{1}$$

where n_f is the refractive index of the glass optical fiber (1.46), and n_w is the refractive index of water (1.33) at 25 °C.[24] Under ultrasonic wave radiation, the resulting Δn gives the reflection ratio of the light intensity (R_{on}),

$$R_{on} = \left(\frac{n_f - n_w + \Delta n}{n_f + n_w}\right)^2 \cong \left(\frac{n_f - n_w}{n_f + n_w}\right)^2 + 2\frac{n_f - n_w}{n_f + n_w}\frac{\Delta n}{n_f + n_w}, \tag{2}$$

where Δn is much smaller than the refractive index of water n_w. By measuring the Fresnel reflected light intensity from the end surface of the optical fiber before and during ultrasonic wave radiation, it is possible to estimate the Δn as

$$\frac{R_{on}-R_{off}}{R_{off}}=\frac{2\Delta n}{n_f-n_w} \iff \Delta n=\frac{(n_f-n_w)(R_{on}-R_{off})}{2R_{off}}. \quad (3)$$

The distribution of Δn is measured from 0.2 to 1.0 mm in the sound-axis direction from the center of the transducer surface. At the sound-axis position of 0 to 0.2 mm, measurement is difficult because the presence of the ultrasonic transducer itself affects the probe light from the optical fiber. Figure 3(b) shows the sound-axis distribution of Δn at 160 MHz and input voltage of 92 V_{pp}. The error bars are the standard deviations of the three measurements, and the plots represent their mean values. The vertical axis indicates the Δn caused by ultrasonic radiation. The result in Fig. 3(b) shows that Δn, induced by high-frequency high-intensity ultrasonic radiation, approaches a smaller refractive index (i.e., the refractive index of air) and the distribution of Δn along the sound-axis direction, with Δn decreasing as the distance from the transducer surface increases. The measurement results from the fiber optic probe show that the average and maximum Δn are approximately 0.04 and 0.06 at respective distances of 0.20 to 0.52 mm from the transducer surface. Although the measured values vary widely at 0.48 and 0.52 mm, we attribute this to temporal fluctuations at the tip of the fiber optic sensor caused by acoustic streaming generated in the water by the high-frequency ultrasonic waves.[25] The boundary between the near and far sound fields can be calculated with the following equation: $Z \approx a^2/\lambda = 4.26 \times 10^2$ mm, where λ is the ultrasonic radiation wavelength, and a is the ultrasonic radiation source radius. This indicates that the Δn formed by ultrasonic radiation is within the near field.

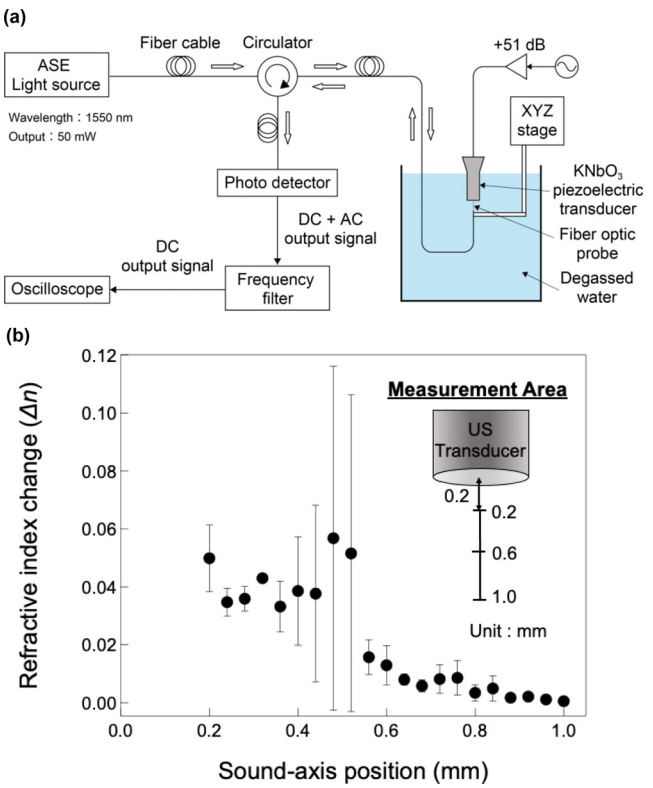

FIG. 3. Refractive index distributions measured by a fiber optic probe. (a) Block diagram of the fiber optic probe measurement system. (b) The sound-axis distributions of the refractive index change (Δn) under ultrasonic radiation at 160 MHz and 92 V_{pp} measured by a fiber optic probe. Plots and error bars indicate the mean values and standard deviations ($n = 3$).

The mechanism of the static change of refractive index induced by high-frequency, high-intensity ultrasonic radiation has two potential factors: cavitation bubbles and thermal effects. The first factor is the possibility of *acoustic cavitation*, a well-known phenomenon wherein micrometer-sized bubbles are generated in liquids from bubble nuclei by a high-intensity ultrasonic field.[26] The behavior of microbubbles is dependent on ultrasonic parameters such as the sound pressure amplitude and frequency. Cavitation generation of megahertz-range ultrasonic waves has often been reported in the literature, and the cavitation threshold of the sound pressure is known to be dependent on ultrasonic frequency.[27–29] A higher sound frequency gives a higher cavitation threshold. However, cavitation phenomena under high-frequency, high-intensity ultrasonic waves over 100 MHz have not been well studied, and a theoretical model for acoustic cavitation generation has yet to be established. We have recently observed acoustic cavitation under ultrasonic radiation at 10 MHz using a $KNbO_3$ ultrasonic transducer by sonoluminescence reaction (supplementary material). Figure 3(b) shows that a spatial refractive index distribution is formed by ultrasonic radiation, and if the refractive index is modulated by acoustic cavitation, this refractive index gradient may correspond to the number density gradient of the acoustic cavitation bubbles. In the case of $\Delta n = 0.06$, the volume fraction of air in water can be estimated simply to be 17%. Additionally, we have attempted to radiate high-frequency, high-intensity ultrasonic waves into solids (quartz glass) using $KNbO_3$ ultrasonic transducers, but the same phenomenon observed in liquids has not yet been confirmed. Further investigation on cavitation generation will be discussed in future, considering that acoustic cavitation may also occur near the transducer surface with radiation of high-intensity ultrasonic waves in the 100 MHz range. The second possible factor is the thermal effect caused by ultrasonic wave attenuation. Ultrasonic waves with strong nonlinearity at higher frequencies give a larger absorption attenuation for wave propagation,[30] resulting in a larger temperature rise in the medium (water) through conversion of the ultrasonic energy to thermal energy. The temperature rise in water causes a decrease in the density of water, leading to a decrease in the refractive index. The temperature rise in water by ultrasonic radiation was evaluated using a thermography camera and a sheathed platinum resistance thermometer (supplementary material), indicating that the temperature rise in water close to the ultrasonic transducer was within a few degrees at $t = 5.4$ s. Schiebener *et al.* have reported that the theoretical calculation of the refractive index of water changed by temperature.[31] According to theoretical estimations, even if the temperature of water rises to 90 °C by ultrasonic radiation at atmospheric pressure, the change in refractive index Δn will be less than 0.01. This means that the ultrasonic thermal effect should contribute somewhat to the decrease in refractive index but is not the main factor for the present change in our data.

In conclusion, we report a giant static refractive index gradient in liquid induced by high-frequency, high-intensity (in the 100-megahertz-range, on the order of megapascals) ultrasonic radiation. We consider that the main physical mechanism of this phenomenon is likely to be related to acoustic cavitation caused by ultrasonic radiation.

In future work, we will fabricate AO devices with a more suitable design for high-frequency, high-intensity ultrasonic wave propagation using the $KNbO_3$ piezoelectric film, which can be applied to optical device technology.

See the supplementary material for laser beam deflection by ultrasonic radiation, spatial distribution of refractive index change, refractive index change area captured by Schlieren photography (movie), evaluation of temperature rise in water by ultrasonic radiation, and sonoluminescence caused by ultrasonic radiation.

This work was supported by JSPS KAKENHI Grant No. 22H01391, Grant-in-Aid for JSPS Fellows JP23KJ2074, JST SPRING Grant No. JPMJSP2129, Kato Foundation for Promotion of Science, the Casio Science Promotion Foundation, Suzuken Memorial Foundation, and Tateisi Science and Technology Foundation. We thank Dr. Yoshiaki Watanabe for his valuable suggestions and discussions. We are also grateful to M. Hammonds, Ph.D., from Edanz (https://jp.edanz.com/ac) for editing the draft of this manuscript.

AUTHOR DECLARATIONS

Conflict of Interest

The authors have no conflicts to disclose.

Author Contributions

Yuki Harada: Conceptualization (equal); Data curation (equal); Formal analysis (lead); Funding acquisition (equal); Investigation (lead); Methodology (lead); Resources (equal); Software (equal); Validation (equal); Visualization (lead); Writing – original draft (lead); Writing – review & editing (equal). **Mutsuo Ishikawa:** Conceptualization (equal); Data curation (equal); Investigation (equal); Methodology (equal); Project administration (equal); Resources (equal); Supervision (equal); Writing – original draft (equal); Writing – review & editing (equal). **Yuma Kuroda:** Investigation (supporting); Methodology (supporting); Validation (supporting); Writing – original draft (supporting). **Mami Matsukawa:** Resources (equal); Supervision (equal); Writing – original draft (equal); Writing – review & editing (equal). **Daisuke Koyama:** Conceptualization (equal); Data curation (equal); Formal analysis (equal); Funding acquisition (lead); Methodology (equal); Project administration (lead); Resources (lead); Supervision (lead); Validation (lead); Visualization (equal); Writing – original draft (equal); Writing – review & editing (lead).

DATA AVAILABILITY

The data that support the findings of this study are available from the corresponding author upon reasonable request.

REFERENCES

[1]G. Duemani Reddy, K. Kelleher, R. Fink, and P. Saggau, "Three-dimensional random access multiphoton microscopy for functional imaging of neuronal activity," Nat. Neurosci. **11**(6), 713–720 (2008).
[2]H. Mikami, J. Harmon, H. Kobayashi, S. Hamad, Y. Wang, O. Iwata, K. Suzuki, T. Ito, Y. Aisaka, N. Kutsuna, K. Nagasawa, H. Watarai, Y. Ozeki, and K. Goda, "Ultrafast confocal fluorescence microscopy beyond the fluorescence lifetime limit," Optica **5**(2), 117 (2018).
[3]L. Kong, J. Tang, J. P. Little, Y. Yu, T. Lämmermann, C. P. Lin, R. N. Germain, and M. Cui, "Continuous volumetric imaging via an optical phase-locked ultrasound lens," Nat. Methods **12**(8), 759–762 (2015).
[4]T.-H. Chen, R. Fardel, and C. B. Arnold, "Ultrafast z-scanning for high-efficiency laser micro-machining," Light: Sci. Appl. **7**(4), 17181 (2018).
[5]M. Chamanzar, M. G. Scopelliti, J. Bloch, N. Do, M. Huh, D. Seo, J. Iafrati, V. S. Sohal, M.-R. Alam, and M. M. Maharbiz, "Ultrasonic sculpting of virtual optical waveguides in tissue," Nat. Commun. **10**(1), 92 (2019).
[6]S. Taniguchi, D. Koyama, Y. Shimizu, A. Emoto, K. Nakamura, and M. Matsukawa, "Control of liquid crystal molecular orientation using ultrasound vibration," Appl. Phys. Lett. **108**(10), 101103 (2016).
[7]Y. Shimizu, D. Koyama, S. Taniguchi, A. Emoto, K. Nakamura, and M. Matsukawa, "Periodic pattern of liquid crystal molecular orientation induced by ultrasound vibrations," Appl. Phys. Lett. **111**(23), 231101 (2017).
[8]Y. Shimizu, D. Koyama, M. Fukui, A. Emoto, K. Nakamura, and M. Matsukawa, "Ultrasound liquid crystal lens," Appl. Phys. Lett. **112**(16), 161104 (2018).
[9]Y. Harada, D. Koyama, M. Fukui, A. Emoto, K. Nakamura, and M. Matsukawa, "Molecular orientation in a variable-focus liquid crystal lens induced by ultrasound vibration," Sci. Rep. **10**(1), 6168 (2020).
[10]J. Onaka, T. Iwase, M. Fukui, D. Koyama, and M. Matsukawa, "Ultrasound liquid crystal lens with enlarged aperture using traveling waves," Opt. Lett. **46**(5), 1169 (2021).
[11]X. Dai, H. Yang, T. Shan, H. Xie, S. A. Berceli, and H. Jiang, "Miniature endoscope for multimodal imaging," ACS Photonics **4**(1), 174–180 (2017).
[12]H. Pahlevaninezhad, M. Khorasaninejad, Y.-W. Huang, Z. Shi, L. P. Hariri, D. C. Adams, V. Ding, A. Zhu, C.-W. Qiu, F. Capasso, and M. J. Suter, "Nano-optic endoscope for high-resolution optical coherence tomography in vivo," Nat. Photonics **12**(9), 540–547 (2018).
[13]Y. Liang, W. Fu, Q. Li, X. Chen, H. Sun, L. Wang, L. Jin, W. Huang, and B.-O. Guan, "Optical-resolution functional gastrointestinal photoacoustic endoscopy based on optical heterodyne detection of ultrasound," Nat. Commun. **13**(1), 7604 (2022).
[14]Y. Yang, A. Q. Liu, L. K. Chin, X. M. Zhang, D. P. Tsai, C. L. Lin, C. Lu, G. P. Wang, and N. I. Zheludev, "Optofluidic waveguide as a transformation optics device for lightwave bending and manipulation," Nat. Commun. **3**(1), 651 (2012).
[15]H. L. Liu, X. Q. Zhu, L. Liang, X. M. Zhang, and Y. Yang, "Tunable transformation optical waveguide bends in liquid," Optica **4**(8), 839 (2017).
[16]M. G. Scopelliti, H. Huang, A. Pediredla, S. G. Narasimhan, I. Gkioulekas, and M. Chamanzar, "Overcoming the tradeoff between confinement and focal distance using virtual ultrasonic optical waveguides," Opt. Express **28**(25), 37459 (2020).
[17]G. Huang, V. A. Bolaños Quiñones, F. Ding, S. Kiravittaya, Y. Mei, and O. G. Schmidt, "Rolled-up optical microcavities with subwavelength wall thicknesses for enhanced liquid sensing applications," ACS Nano **4**(6), 3123–3130 (2010).
[18]H. L. Liu, Y. Shi, L. Liang, L. Li, S. S. Guo, L. Yin, and Y. Yang, "A liquid thermal gradient refractive index lens and using it to trap single living cell in flowing environments," Lab Chip **17**(7), 1280–1286 (2017).
[19]M. Ishikawa, H. Einishi, M. Nakajima, T. Hasegawa, T. Morita, Y. Saijo, M. Kurosawa, and H. Funakubo, "Effect of deposition time on film thickness and their properties for hydrothermally-grown epitaxial $KNbO_3$ thick films," Jpn. J. Appl. Phys., Part 1 **49**(7S), 07HF01 (2010).
[20]T. Neumann and H. Ermert, "Schlieren visualization of ultrasonic wave fields with high spatial resolution," Ultrasonics **44**, e1561–e1566 (2006).
[21]J. Staudenraus and W. Eisenmenger, "Fibre-optic probe hydrophone for ultrasonic and shock-wave measurements in water," Ultrasonics **31**(4), 267–273 (1993).
[22]P. Huber, J. Debus, P. Peschke, E. W. Hahn, and W. J. Lorenz, "*In vivo* detection of ultrasonically induced cavitation by a fibre-optic technique," Ultrasound Med. Biol. **20**(8), 811–825 (1994).
[23]H. Takei, T. Hasegawa, K. Nakamura, and S. Ueha, "Measurement of intense ultrasound field in air using fiber optic probe," Jpn. J. Appl. Phys., Part 1 **46**(7B), 4555–4557 (2007).
[24]G. M. Hale and M. R. Querry, "Optical constants of water in the 200-nm to 200-μm wavelength region," Appl. Opt. **12**, 555–563 (1973).

[25]T. M. Squires and S. R. Quake, "Microfluidics: Fluid physics at the nanoliter scale," Rev. Mod. Phys. **77**(3), 977–1026 (2005).
[26]E. A. Neppiras, "Acoustic cavitation," Phys. Rep. **61**(3), 159–251 (1980).
[27]R. E. Apfel and C. K. Holland, "Gauging the likelihood of cavitation from short-pulse, low-duty cycle diagnostic ultrasound," Ultrasound Med. Biol. **17**(2), 179–185 (1991).
[28]A. Brotchie, F. Grieser, and M. Ashokkumar, "Effect of power and frequency on bubble-size distributions in acoustic cavitation," Phys. Rev. Lett. **102**(8), 084302 (2009).
[29]T. Thanh Nguyen, Y. Asakura, S. Koda, and K. Yasuda, "Dependence of cavitation, chemical effect, and mechanical effect thresholds on ultrasonic frequency," Ultrason. Sonochem. **39**, 301–306 (2017).
[30]J. M. M. Pinkerton, "The absorption of ultrasonic waves in liquids and its relation to molecular constitution," Proc. Phys. Soc. B **62**(2), 129–141 (1949).
[31]P. Schiebener, J. Straub, J. M. H. Levelt Sengers, and J. S. Gallagher, "Refractive index of water and steam as function of wavelength, temperature and density," J. Phys. Chem. Ref. Data **19**(3), 677–717 (1990).